Journal of the Serbian Chemical Society
JSCS-info@shd.org.rs • www.shd.org.rs/JSCS
J. Serb. Chem. Soc. 77 (9) 1223–1237 (2012)
JSCS–4347
UDC 667.282.4+667.287:
544.6.004.12:537.872
Original scientific paper

Synthesis and photovoltaic properties of octacarboxy-metallophthalocyanine dyes applied in dye-sensitized solar cells

LING JIN, WEI CHEN and DAJUN CHEN*

State Key Laboratory for Modification of Chemical Fibers and Polymer Materials, College of Materials Science and Engineering, Donghua University, Shanghai 201620, China

(Received 10 July 2011, revised 19 March 2012)

Abstract: A series of octacarboxy-metallophthalocyanine dyes with different central metal ions, *i.e.*, MgOCPc, MnOCPc, FeOCPc and ZnOCPc, were designed and synthesized by microwave irradiation. The effects of the introduction of different metal ions with variant 3d orbitals ($3d^0$, $3d^5$, $3d^6$, and $3d^{10}$, respectively) in the centre of the phthalocyanine rings on the thermal, photophysical, and electrochemical properties of octacarboxy-metallophthalocyanines were characterized and evaluated in detail. The results showed that ZnOCPc and MgOCPc, with closed-shell metal ions, and FeOCPc, with an open-shell metal ion, had excellent thermal properties. However, MnOCPc, with a half-full-shell metal ion, exhibited the lowest decomposition temperature and largest Q-band red shifts. The energy gaps of MgOCPc, MnOCPc, FeOCPc and ZnOCPc were theoretically calculated to be 0.11, 0.10, 0.20 and 0.22V, respectively. Applied in TiO_2 nanocrystalline dye-sensitized solar cells (DSSC), the photovoltaic properties of the four dyes were obtained under AM1.5 irradiation (100 mW cm^{-2}).

Keywords: octacarboxy-metallophthalocyanine dyes; 3d orbital; photophysical properties; electrochemical properties; energy gaps; DSSC.

INTRODUCTION

Owing to their extensively delocalized 18-π electron system consisting of four isoindole subunits linked together through nitrogen atoms,[1,2] phthalocyanines (Pcs) possess interesting properties, such as high thermal and chemical stability, efficient light absorption from the red to the near infrared region(NIR) of the optical spectrum, and both semi- and photoconducting characteristic.[3] Pcs and their metallo-derivatives have received considerable attention in recent years and have been intensively applied as optical recording media,[4] liquid crystals,[5]

* Corresponding author. E-mail: cdj@dhu.edu.cn
doi: 10.2298/JSC110710026J

photodynamic therapy for cancer,[6] nonlinear optical materials (NLO),[7] electrocatalytic detection,[8] photovoltaic cells[9–11] and many other fields.

Pcs are of interest as NIR photosensitizers for employment in dye-sensitized solar cells (DSSC) due to their above-mentioned excellent properties. DSSC are based on photo-induced electron injection from excited molecules into the conduction band of a nanocrystalline metal oxide film.[1] Thus, the current is generated when photons absorbed by dye molecules that are placed over a layer of a wide band-gap semiconducting material such as a mesoporous metal oxide, *e.g.*, TiO_2.[1,12] However, for a long time, the applications of Pc dyes in DSSC was restricted due to their poor solubility in organic solvents and other factors.[13] To improve their water solubility, Pcs were functionalized with carboxy-,[14–17], sulfo-[9] and ester groups.[18] Grätzel and Nazeeruddin *et al*.[9] reported on the use of different substituted zinc(II) and aluminum(III) phthalocyanines using the tetracarboxylate functionality as efficient charge transfer sensitizers. They and Hagfeldt *et al*.[14] designed a new type of zinc phthalocyanines with tyrosine substituents (ZnPcTyr) and glycine substituents (ZnPcGly) to make the dyes ethanol-soluble and enhance significantly the solar cell performance. Boston[19] and co-workers first reported the synthesis of copper phthalocyanine octacarboxylic acid. Matemadombo and Nyokong[20] used cobalt octacarboxy phthalocyanine (CoOCPc) adsorbed onto glassy carbon electrodes for the electrocatalytic detection of nitrite, L-cysteine and melatonin. Masilela and Nyokong[21] synthesized water-soluble octacarboxylated Ga phthalocyanine and discussed its photophysical properties. However, there are hardly any reports describing the application of octacarboxy-metallophthalocyanines for DSSC.

Conventional heating methods, involving the use of an oil bath or muffle furnace that heat the reactor wall by convection, result in slow and time-consuming syntheses of metallophthalocyanines. However, using a microwave heating system, which is able to heat target compounds and produce more uniform thermal energy making molecules dramatically collide, heat is generated from inside the target compounds in contrast with the conventional heating methods where heat is transferred from outside to inside.[22,23] Thus, the synthesis time is remarkably reduced and the yield of reaction product greatly increased when a microwave heating system is employed.

In this work, four octacarboxy-metallophthalocyanine dyes (MOCPc) containing different central metals (Mg, Mn, Fe and Zn) were designed and synthesized by microwave irradiation. Herein, the effect of the introduction of different metal ions with variant 3d orbitals ($3d^0$, $3d^5$, $3d^6$ and $3d^{10}$, respectively) in the centre of the phthalocyanine rings on the thermal, photophysical and electrochemical properties of octacarboxy-metallophtalocyanines were investigated. Moreover, the four dyes were applied in nanocrystalline TiO_2–dye-sensitized solar cells and their photovoltamic performances were measured.

EXPERIMENTAL

Materials

Pyromellitic dianhydride, urea, hexaammonium heptamolybdate tetrahydrate, zinc chloride, iron(II) chloride tetrahydrate, manganese(II) chloride tetrahydrate, magnesium chloride hexahydrate, potassium hydroxide, tetrabutylammonium perchlorate (TBAP) and hydrochloric acid (37 %) of analytical grade were purchased from Sinopharm Chemical Reagent Co., Ltd.. The acetone and dimethylsulfoxide (DMSO) used in this work were of reagent grade and were used without further purification.

Synthesis of the octacarboxy-metallophthalocyanine dyes

The MOCPc were synthesized by microwave irradiation from pyromellitic dianhydride, metal halide and urea, as shown in Scheme 1.

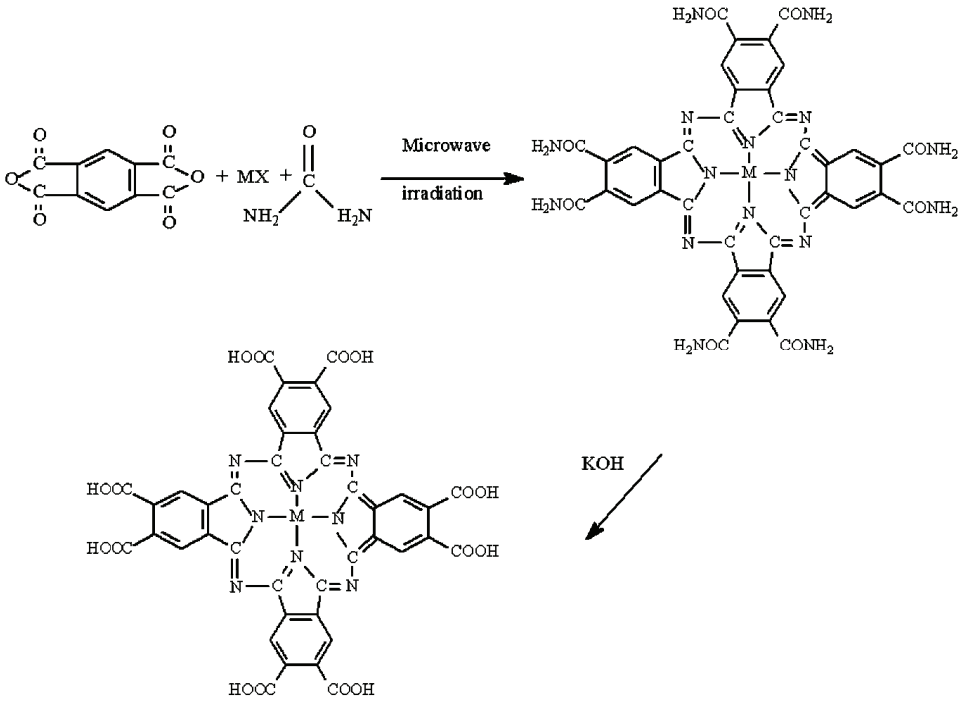

Scheme 1. Molecular structures and synthesis of the octacarboxy-metallophthalocyanine dyes.

Synthesis of octacarboxy-metallophthalocyanine of zinc: pyromellitic dianhydride (5.05 g, 23.1 mmol), urea (26.0 g, 0.430 mol), $ZnCl_2$ (6.28 g, 46.2 mmol) and hexaammonium heptamolybdate tetrahydrate (0.2 g) were ground together in a 500 ml beaker and irradiated in a microwave oven at 320 W for 10 min. The black solid was then cooled and washed with water, acetone, and dried in air. Next, the crushed solid was stirred in 6 M HCl solution (200 ml) for 30 min. This procedure was repeated three times and the supernatant liquid was decanted each time. Finally, the solid was hydrolyzed in 10 % NaOH water solution (250 ml), and the mixture was heated for 8–10 h at 85 °C with stirring. The reaction mixture was then diluted with distilled water (100 ml), filtered through a No. 5 sintered glass funnel, and the

filtrate was slowly acidified to pH ≥ 3 with concentrated HCl (12 M). At this point, the product completely precipitated as a blue, flocculent solid and was washed with the distilled water and acetone until the mixture solution was a clear color. This was allowed to settle, and most of the supernatant liquid was decanted. The blue product that precipitated was separated from the liquor using a centrifuge and then dried in a vacuum drying oven at 30 °C. The solid reaction product was quite soluble in water, although it dissolved slowly, and somewhat soluble in acetone. It was, however, insoluble in acidic aqueous solutions. The same procedure was adopted in the preparation of the respective magnesium, manganese, and iron octacarboxy phthalocyanines, M(OCPc) (M = Mn or Fe). Their IR spectra and NMR spectra were similar to those of ZnOCPc.

Characterizations

IR spectra (KBr pellets) were recorded on a Nicolet 8700 FTIR spectrometer. ^{1}H-NMR spectra were obtained using a Bruker AV 400 MHz NMR spectrometer. Thermal properties were tested on an Iris 209 F1 thermo gravimetric analyzer at a heating rate of 10 °C min^{-1} under nitrogen. The UV–Vis spectra were investigated on a Lambda A35 UV–Vis/NIR spectrophotometer. Fluorescence excitation and emission spectra were recorded on a FP-6600 spectrofluorometer. The samples were contained in 1 cm path-length quartz cells. The electrochemical properties were measured with a CIMPS-1 electrochemical workstation. In addition, cyclic voltammetry measurements (CV) were realized in a three-electrode measuring cell with a glassy carbon working electrode, a Pt wire counter electrode and an Hg/Hg_2Cl_2 reference electrode. The supporting electrolyte was 0.1 M TBAP in DMSO.

ZnOCPc. Yield: 35 %; Anal. Calcd. for $C_{40}H_{16}N_8O_{16}Zn$ ($16H_2O$): C, 40.51; H, 4.05; N, 9.45 %. Found: C, 39.11; H, 3.83; N, 8.53 %; IR (KBr, cm^{-1}): 3388 (O–H stretching of COOH group), 3144 (C–H stretching of aromatic ring), 1701 (C=O stretching of COOH group), 1302 (C–O stretching of COOH group), 1624 (C=N or C=C stretching of phthalocyanine ring), 1353, 1094 (C–C or C–N stretching of phthalocyanine ring), 739 (C–H stretching of aromatic ring); ^{1}H-NMR (400 MHz, DMSO-d_6, δ / ppm): 8.78 (8H, *s*, terminal phenyl), 10.07 (8H, *s*, COOH); ^{13}C-NMR (100 MHz, DMSO-d_6, δ / ppm): 138.30 (C_{quat}), 136.43 (C_{quat}), 171.44 (COO), 171.13 (COO), 170.08 (COO), 169.46 (COO), 155.94 (CN), 142.99 (CN), 141.25 (CN), 128.80 (CH), 128.03 (CH).

FeOCPc. Yield: 40 %; Anal. Calcd. for $C_{40}H_{16}N_8O_{16}Fe$ ($16H_2O$): C, 40.82; H, 4.08; N, 9.52 %. Found: C, 39.32; H, 3.93; N, 8.69 %; IR (KBr, cm^{-1}): 3398 (O–H stretching of COOH group), 3168 (C–H stretching of aromatic ring), 1710 (C=O stretching of COOH group), 1312 (C–O stretching of COOH group), 1620 (C=N or C=C stretching of phthalocyanine ring), 1359, 1094 (C–C or C–N stretching of phthalocyanine ring), 748 (C–H stretching of aromatic ring).

MnOCPc. Yield: 25 %; Anal. Calcd. for $C_{40}H_{16}N_8O_{16}Mn$ ($16H_2O$): C, 40.85; H, 4.09; N, 9.53 %. Found: C, 39.37; H, 3.92; N, 8.63 %; IR (KBr, cm^{-1}): 3406 (O–H stretching of COOH group), 3163 (C–H stretching of aromatic ring), 1702 (C=O stretching of COOH group), 1304 (C–O stretching of COOH group), 1623 (C=N or C=C stretching of phthalocyanine ring), 1362, 1088 (C–C or C–N stretching of phthalocyanine ring), 719 (C–H stretching of aromatic ring).

MgOCPc. Yield: 15%; Anal. Calcd. for $C_{40}H_{16}N_8O_{16}Mg$ ($16H_2O$): C, 41.96; H, 4.20; N, 9.79 %. Found: C, 40.31; H, 3.98; N, 8.78 %; IR (KBr, cm^{-1}): 3415 (O–H stretching of COOH group), 3169 (C–H stretching of aromatic ring), 1706 (C=O stretching of COOH group), 1304 (C–O stretching of COOH group), 1621 (C=N or C=C stretching of phthalocyanine ring), 1358, 1083 (C–C or C–N stretching of phthalocyanine ring), 735 (C–H stretch-

ing of aromatic ring); ^{1}H-NMR (400 MHz, DMSO-d_6, δ / ppm): 7.50 (8H, *s*, terminal phenyl), 9.76 (8H, *s*, COOH); ^{13}C-NMR (100 MHz, DMSO-d_6, δ / ppm): 138.04 (C_{quat}), 170.97 (COO), 170.04 (COO), 169.68 (COO), 152.68 (CN), 127.70 (CH).

Fabrication of dye-sensitized solar cells

The DSSC consisted of a dye-adsorbed TiO_2 electrode, a counter electrode, and an organic electrolyte. The electrolyte solution was a mixture of DMPII/LiI/I_2/TBP/GuSCN. The TiO_2 electrodes with a 0.23 cm^2 working area were purchased from Dalian HeptaChroma Solar-Tech Co. They were heated at 450 °C for 30 min and then allowed to cool to 80–90 °C before immersion in the dye solutions. The dye solutions were prepared in DMSO at a concentration of 1.8×10^{-5} M. The TiO_2 electrodes were immersed into the dye solutions for 6 h at room temperature. Finally, the dye-adsorbed TiO_2 electrodes were rinsed several times with DMSO and ethanol to remove non-adsorbed dye and then dried quickly under a N_2 flow. As a counter electrode, a thin Pt layer was deposited on FTO conducting glass. The photovoltaic performance of the DSSC device was measured using a Keithley 2400 digital source meter under 100 mW cm^{-2} simulated air mass (AM) 1.5 solar light illumination.

The fill factor (*FF*) is defined by the following equation:[24]

$$FF = j_m V_m / j_{sc} V_{oc} \quad (1)$$

where j_m and V_m are the photocurrent density and voltage for maximum power output, respectively, and j_{sc} and V_{oc} are the short circuit photocurrent density and open circuit voltage, respectively.

The solar energy-to-electricity conversion efficiency (η) of a DSSC is calculated from j_{sc}, V_{oc}, *FF* and the intensity of the incident light (P_{in}) according to the following equation:[25]

$$\eta = j_{sc} V_{oc} FF / P_{in} \quad (2)$$

RESULTS AND DISCUSSION

Thermal properties

The incorporation of a metal ion into the central cavity affects thermal stability of phthalocyanines, which could be due to how different metals interact with phthalocyanine rings. The thermal properties of the four dyes are shown in Fig. 1. The valence electron distribution and ionic radius of metal ion and the data of the decomposition temperature of the four dyes are collected in Table I. The decomposition temperature of MnOCPc with a half-full-shell metal ion is lower than that of the other dyes. As Table 1 shows, the ionic radius of Mn^{2+} with a $3d^5$ orbital is the largest, which may result in the central metal interacting weakly with the phthalocyanine ring giving rise to the lowest decomposition temperature.[26–28] The decomposition temperature of FeOCPc with an open-shell metal ion is the highest due to the strong interaction between the metal and the Pc ligand. On the other hand, ZnOCPc and MgOCPc with closed-shell metal ions may form outer-orbital complexes, while FeOCPc is an inner-orbital complex, which leads to the thermal stability of ZnOCPc and MgOCPc being slightly lower than that of FeOCPc.

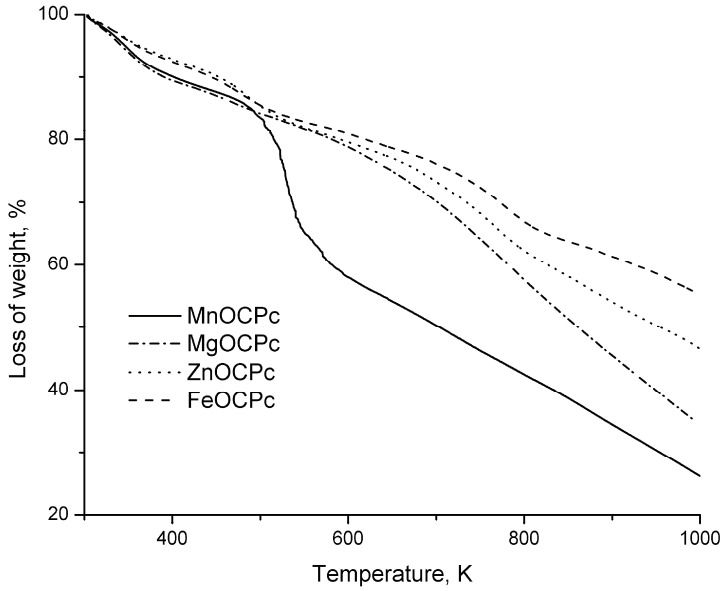

Fig. 1. Thermal properties of the four dyes.

TABLE I. Valance electron distribution of the metal ion and thermal decomposition temperature of the four dyes

Dye	Metal ion	Ionic radius pm	Valence electron distribution	Decomposition temperature, K
MgOCPc	Mg^{2+}	66	$1s^2 2s^2 2p^6$	748
MnOCPc	Mn^{2+}	90	$1s^2 2s^2 2p^6 3d^5$	529
FeOCPc	Fe^{2+}	85	$1s^2 2s^2 2p^6 3d^6$	777
ZnOCPc	Zn^{2+}	83	$1s^2 2s^2 2p^6 3d^{10}$	765

Photophysical properties

The UV–Vis spectra of the octacarboxy-metallophthalocyanine dyes in DMSO solution are displayed in Fig. 2, and the Q band maximum absorption wavelength and the molar extinction coefficient of the four dyes are summarized in Table II.

The absorption bands of the four as-synthesized dyes are similar and exhibit the features typical of a phthalocyanine ring, with a Soret band (B-band) in the range 300–400 nm. The Q band in the NIR region 600–800 nm is assigned to a ligand-centered π–π^* transition from the highest occupied molecular orbital (HOMO) to the lowest unoccupied molecular orbital (LUMO) in the main conjugation system of the phthalocyanine macro-ring. The position of the Q band and the shape of the spectral curve are determined by the nature of the metal, substituents on the benzene rings, solvent, concentration, and other factors.[29] It is evident that the Q bands of the four dyes have different red shifts following the

order MnOCPc > MgOCPc > ZnOCPc > FeOCPc. In DMSO, the absorption spectrum of MnOCPc has a Q band peak at 725 nm, while the Q band of MnOCPc is strongly red-shifted 38 nm when compared to FeOCPc and 22 nm when compared to that of MgOCPc. The observed red shifts could be attributed to the linear combination of the atomic orbitals (LCAO) coefficient in MnOCPc of the HOMO being greater than are those of ZnOCPc and FeOCPc, resulting in the HOMO level of MnOCPc being destabilized more than are those of ZnOCPc and FeOCPc. As a result, the energy gap between the HOMO and LOMO becomes smaller leading to the generated red shifts.

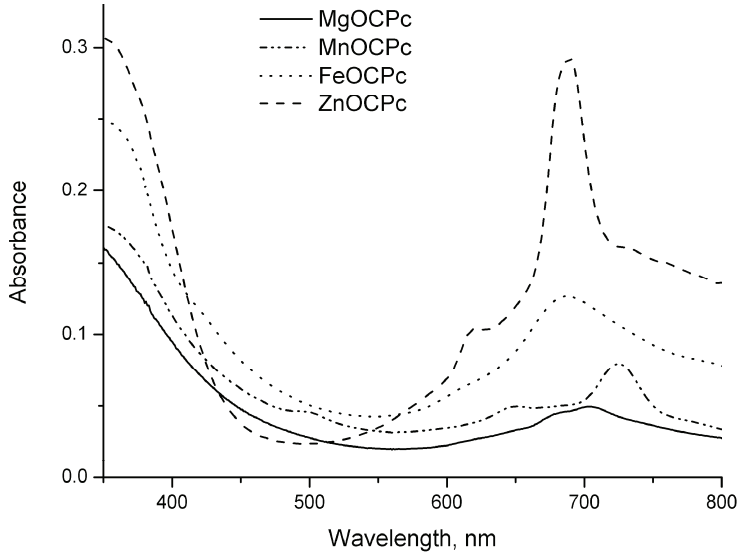

Fig. 2. UV–Vis absorption spectra of the four dyes in DMSO solution at concentrations of about 7.2×10^{-6} M.

TABLE II. The absorption and the molar extinction coefficient data for the four dyes

Dye	Q band, λ_{max} / nm	ε_{max}[a] / M^{-1} cm^{-1}
MgOCPc	703	6856
MnOCPc	725	11022
FeOCPc	687	17576
ZnOCPc	689	40697

[a]ε_{max} is the molar extinction coefficient at λ_{max} of absorption

The four dyes (MgOCPc, MnOCPc, FeOCPc and ZnOCPc) showed similar fluorescence behavior in DMSO. The fluorescence emission and excitation spectra for the four dyes measured in DMSO are shown in Fig. 3 and the maximum emission and excitation data are summarized in Table III. In DMSO, the emission peaks were observed at 709 (MgOCPc), 725 (MnOCPc), 695 (FeOCPc) and

698 nm (ZnOCPc). The excitation spectra of the four dyes were mirror images of the fluorescent spectra in DMSO except for the spectra of MnOCPc. This can be explained by MnOCPc as an intermediate-spin complex[26] has an unable excitation state. The observed Stokes shift were typical of the four dyes in DMSO and were similar, *i.e.*, 6 (MgOCPc), 5 (MnOCPc), 6 (FeOCPc) and 9 nm (ZnOCPc).

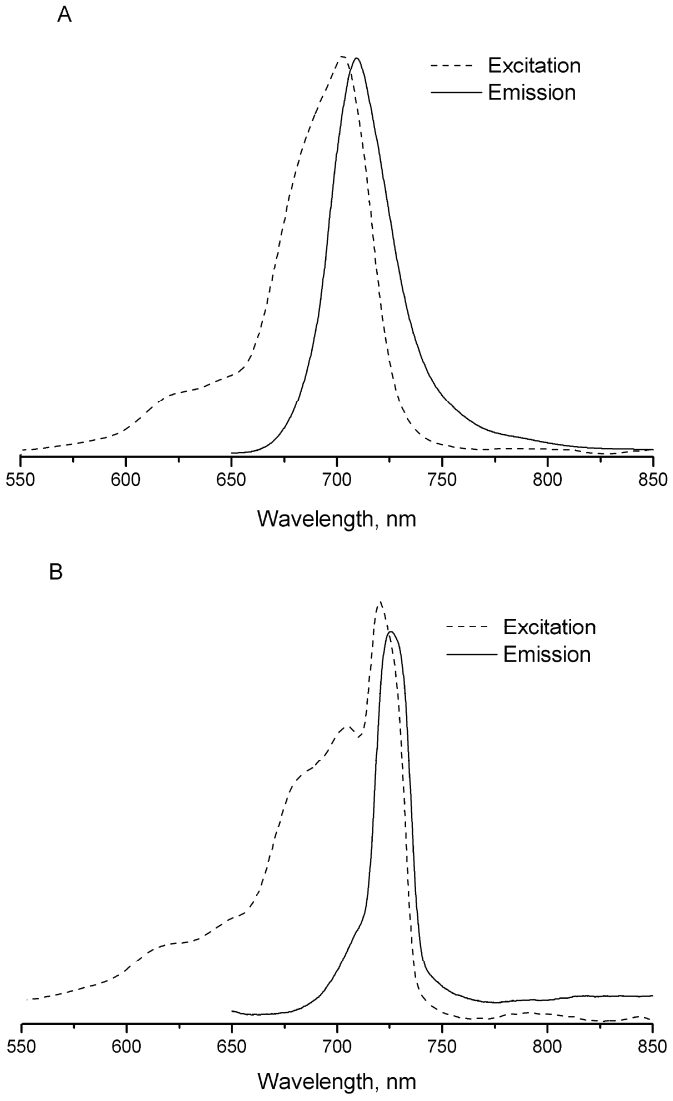

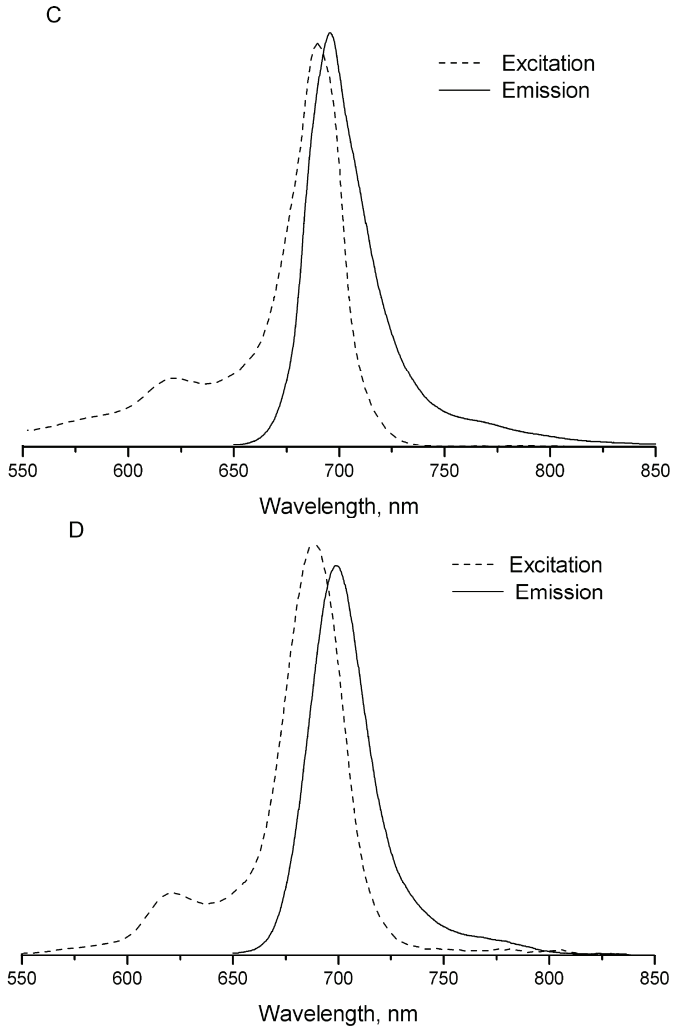

Fig. 3. Emission and excitation spectra of the four dyes in DMSO solution: A) MgOCPc; B) MnOCPc; C) FeOCPc; D) ZnOCPc. The solution concentrations of samples were about 7.2×10^{-6} M.

TABLE III. Fluorescence emission and excitation spectral parameters of the four dyes

Dye	Emission, λ_{em} / nm	Excitation, λ_{ex} / nm	Stokes shift, Δ_{Stokes}
MgOCPc	709	703	6
MnOCPc	725	720	5
FeOCPc	695	689	6
ZnOCPc	698	689	9

Electrochemical properties

To judge the possibilities of electron transfer from the excited molecules of the dyes to the conduction band of TiO_2 and the regeneration of the dyes, their excited-state redox potentials, which play an important role in the electron-injection process, were measured *via* CV,[30] as shown in Fig. 4. The value can be derived from the ground-state oxidation potential and the zero-zero excitation energy ($E_{(0–0)}$), according to the following equation:

$$E_{(S^+/S^*)} = E_{(S^+/S)} - E_{(0–0)} \quad (3)$$

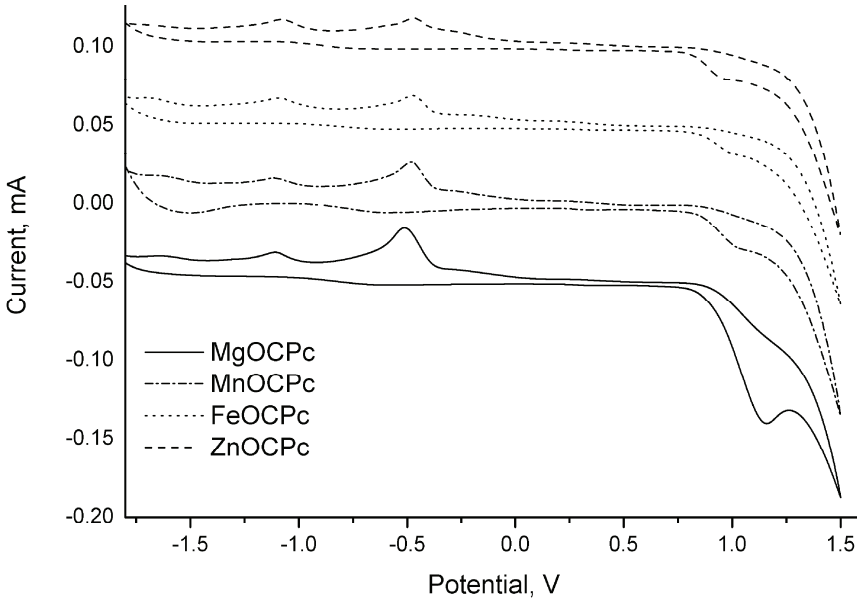

Fig. 4. Electrochemical properties of the four dyes from cyclic voltammetry.

As shown in Table IV, the $E_{(0–0)}$ energies of 1.76, 1.71, 1.79 and 1.78 eV were extracted for MgOCPc, MnOCPc, FeOCPc and ZnOCPc, respectively, from the intersection between the absorption and emission spectra. The energy levels of the four dyes in comparison to the TiO_2 conduction band and the redox couple I^-/I_3^- are illustrated in Fig. 5. It is well known that the efficiency of a dye-sensitized solar cell depends on the balance between the electron injection into the conduction band and the back transfer of injected electrons from the conduction band of TiO_2 to the dye cation radical. The HOMO levels of the four dyes, ranging from 1.15 to 1.06 V *vs*. NHE, were more positive than that of the I^-/I_3^- redox couple (≈ 0.4 V *vs*. NHE), ensuring that sufficient driving force exits for the efficient regeneration of the dyes through the recapture of the injected electrons from I^- by the dyes cation radical.[31] Furthermore, provided that an energy gap of 0.2

eV is necessary for efficient electron injection, these thermodynamic driving forces are sufficient for efficient charge injection. Thus, the electron injection process from the excited dye molecule to the TiO_2 conduction band and the sub-sequent dye regeneration are energetically permitted.[30] From Table IV, it is clear that the energy gaps of MgOCPc, MnOCPc, FeOCPc and ZnOCPc are 0.11, 0.10, 0.20 and 0.22 V, respectively. Therefore, for MgOCPc and MnOCPc the driving force is not sufficient for charge injection from the dyes to the TiO_2 conduction band.

TABLE IV. Electrochemical data for the four dyes

Dye	$E_{(0-0)}$[a] / eV	$E_{(S+/S)}$[b] / V *vs*. NHE	$E_{(S+/S*)}$[c] / V *vs*. NHE	E_{gap}[d] / V
MgOCPc	1.76	1.15	–0.61	0.11
MnOCPc	1.71	1.11	–0.60	0.10
FeOCPc	1.79	1.09	–0.70	0.20
ZnOCPc	1.78	1.06	–0.72	0.22

[a]The E_{0-0} value was calculated from $E_{(0-0)} = 1240/\lambda$, and λ was obtained from the intersection between the absorption and emission spectra; [b]the ground-state energy oxidation potentials ($E_{(S+/S)}$) of the four dyes, describing the highest occupied molecular orbital (HOMO), were measured in DMSO with 0.1 M TBAP as the electrolyte (scanning rate, 30 mV s^{-1}) using glassy carbon as the working electrode, a Pt wire as the counter electrode and an Hg/Hg_2Cl_2 electrode as the reference electrode; [c]the excited state energy ($E_{(S+/S*)}$), reflecting the lowest unoccupied molecular orbital (LUMO); [d]E_{gap} is the energy gap between the $E_{(S+/S*)}$ of the dyes and the conduction band (CB) level of TiO_2 (–0.5 V *vs*. normal hydrogen electrode (NHE))

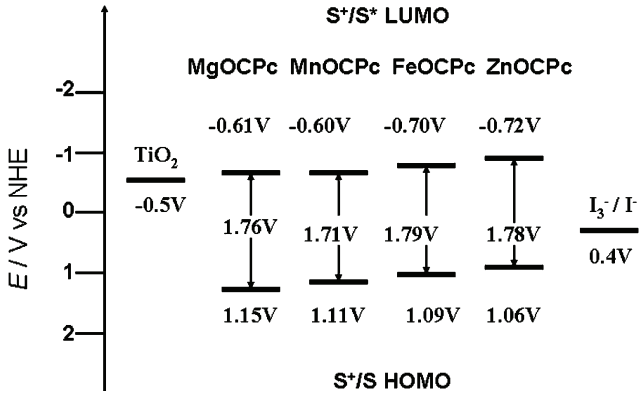

Fig. 5. Energy levels diagram from the electrochemical data.

Photovoltaic performance of DSSC

To manufacture DSSC, the TiO_2 electrodes were immersed into a DMSO solution of the four dyes. The absorption spectra of the four dyes adsorbed on the TiO_2 electrodes are shown in Fig. 6, and the trend of absorption intensity follows the order: ZnOCPc > FeOCPc > MnOCPc > MgOCPc, showing no difference in comparison to the spectra in Fig. 6. However, the spectra were broadened in contrast to the spectra in DMSO solution, which may be ascribed to aggregation of the dyes on the TiO_2 surface.

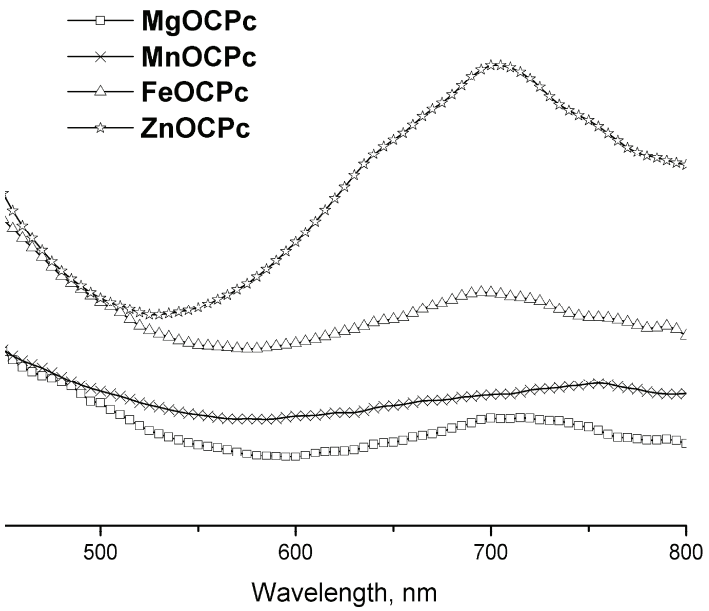

Fig. 6. Absorption spectra of the four dyes adsorbed on TiO_2 electrodes.

The four dye-sensitized TiO_2 electrodes were employed as working electrodes in the DSSC and the effects of the four dyes with different metal ions possessing variant 3d orbital on the photovoltaic performance of the four DSSC devices could be estimated with the aid of photocurrent–voltage characteristics. The *I–V* curves of the DSSCs based on the four dyes are shown in Fig. 7. The detailed parameters are summarized in Table V.

When comparing the photovoltaic performance of the four DSSC devices, it is seen that η assumes the following order: ZnOCPc > FeOCPc > MgOCPc > MnOCPc. The DSSC based on ZnOCPc exhibits the best properties with a short circuit photocurrent density of 0.409 mA cm^{-2}, an open circuit voltage of 0.429 V, and a fill factor of 0.74, corresponding to an overall light to electricity conversion efficiency of 0.13 % under AM 1.5 irradiation (100 mW cm^{-2}). This can be explained by the more negative LUMO level observed for ZnOCPc with the closed-shell metal ion ($3d^{10}$) among the four dyes, which gives a larger driving force for electron injection from this metallophthalocyanine. This trend matches the photovoltaic efficiency trend, which indicates that the factor is crucial to the photovoltaic performance of the DSSC. In addition, ZnOCPc gives stronger absorption than that of the other dyes. However, the MnOCPc-based DSSC device exhibited a lowest efficiency, which is consistent with the lowest j_{sc} value of 0.205 mA cm^{-2} and FF value of 0.60 for this device. The reason is probably due to the poor electron injection and low absorption.

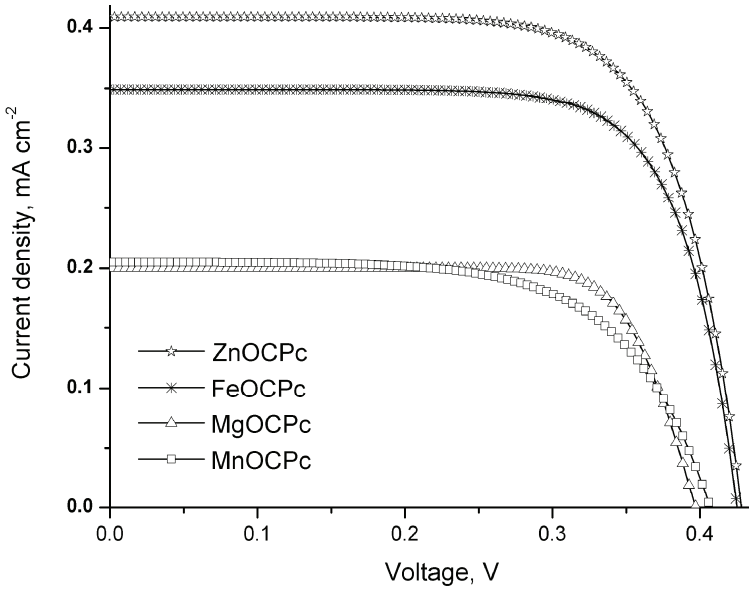

Fig. 7. Current–voltage characteristics for DSSC from the four dyes under illumination of simulated solar light (AM1.5, 100 mW cm^{-2}).

TABLE V. Photovoltaic performance of DSSC based on the four dyes

Dye	j_{sc} / mA cm^{-2}	V_{oc} / V	*FF*	η / %
MgOCPc	0.200	0.397	0.76	0.06
MnOCPc	0.205	0.406	0.60	0.05
FeOCPc	0.348	0.426	0.74	0.11
ZnOCPc	0.409	0.429	0.74	0.13

CONCLUSIONS

In summary, four octacarboxy-metallophthalocyanines (MgOCPc, MnOCPc, FeOCPc and ZnOCPc) were prepared by microwave irradiation, and the resultant dyes possessed excellent solubility in DMSO solution. The decomposition temperature of the four dyes ranged from 256 to 504 °C. The maximum absorption peaks of MnOCPc, FeOCPc and ZnOCPc were all between 687 nm and 725 nm and their red shift wavelength increased with destabilized HOMO of the metal–ligand. Especially, ZnOCPc had a high molar extinction coefficient. Subsequently, the four dyes were anchored to TiO_2 electrodes and their photovoltaic properties applied in DSSC were investigated. It was found that the DSSC device based on ZnOCPc exhibited the best photovoltaic properties with an open circuit voltage of 0.429 V, a short circuit photocurrent density of 0.409 mA cm^{-2} and a fill factor of 0.74 under AM 1.5 irradiation (100 mW cm^{-2}) when compared to the other three dyes. The considerably excellent conversion efficiency obtained with the ZnOCPc-based TiO_2 nanocrystalline dye-sensitized solar cells revealed that

ZnOCPc with a closed-shell metal ion ($3d^{10}$) among the four dyes had an excellent excited state giving the largest driving force for electron injection into the TiO_2 conduction band.

ИЗВОД

СИНТЕЗА И ФОТОНАПОНСКЕ КАРАКТЕРИСТИКЕ ОКТАКАРБОКСИ-МЕТАЛФТАЛОЦИЈАНИНСКИХ БОЈА ЗА ПРИМЕНУ У СОЛАРНИМ ЋЕЛИЈАМА СЕНЗИБИЛИСАНИМ БОЈОМ

LING JIN, WEI CHEN и DAJUN CHEN

State Key Laboratory for Modification of Chemical Fibers and Polymer Materials, College of Materials Science and Engineering, Donghua University, Shanghai 201620, China

Низ октакарбокси-металфталоцијанинских боја са различитм централним јонима метала, MgOCPc, MnOCPc, FeOCPc и ZnOCPc, је дизајниран и синтетисан уз помоћ микроталасног зрачења. Детаљно је испитан утицај увођења металних јона са различитом попуњеношћу 3d орбитала ($3d^0$, $3d^5$, $3d^6$ и $3d^{10}$) у центар фталоцијанинског прстена на термичке, фото-физичке и електрохемијске особине октакарбокси-металфталоцијанина. Резултати су показали да ZnOCPc и MgOCPc који имају метални јон са затвореном љуском и FeOCPc код којег метални јон има отворену љуску поседују одличне термичке особине. Међутим, MnOCPc са металним јоном који има делимично попуњену љуску има најнижу температуру разлагања и највећи црвени померај Q траке. Теоријски је израчунато да енергетски процепи за MgOCPc, MnOCPc, FeOCPc и ZnOCPc износе 0,11, 0,10, 0,20 и 0,22V, респективно. Фотонапонске карактеристике поменуте четири боје, примењене у TiO_2 нанокристалној и бојом сензибилисаној соларној ћелији, одређене су AM1.5 зрачењем снаге 100 mW cm^{-2}.

(Примљено 10. јула 2011, ревидирано 19. марта 2012)

REFERENCES

1. C. G. Claessens, U. Hahn, T. Torres, *Chem. Rec.* **8** (2008) 75
2. N. Masilela, T. Nyokong, *Dyes Pigm.* **84** (2010) 242
3. J. Andzelm, A. M. Rawlett, J. A. Orlicki, J. F. Snyder, *J. Chem. Theory Comput.* **3** (2007) 870
4. M. G. Martín, M. L. Rodríguez-Méndez, J. A. Saja, *Langmuir* **26** (2010) 19217
5. G. Bottari, J. A. Suanzes, O. Trukhina, T. Torres, *J. Phys. Chem. Lett.* **2** (2011) 905
6. M. Kuruppuarachchi, H. Savoie, A. Lowry, C. Alonso, R. W. Boyle, *Mol. Pharmaceutics* **8** (2011) 920
7. G. Torre, P. Vázquez, F. Agulló-López, T. Torres, *Chem. Rev.* **104** (2004) 3723
8. F. Matemadombo, N. Sehlotho, T. Nyokong, *J. Porphyrins Phthalocyanines* **13** (2009) 986
9. M. K. Nazeerruddin, R. Humphry-Baker, M. Grätzel, D. Wöhrle, G. Schnurpfeil, G. Schneider, A. Hirth, N. Trombach, *J. Porphyrins Phthalocyanines* **3** (1999) 230
10. J. J. He, G. Benkö, F. Korodi, T. Polivka, R. Lomoth, B. Åkermark, L. C. Sun, A. Hagfeldt, V. Sundström, *J. Am. Chem. Soc.* **124** (2002) 4922
11. J. J. Cid, J. H. Yum, S. R. Jang, M. K. Nazeeruddin, E. Martínez-Ferrero, E. Palomares, J. Ko, M. Grätzel, T. Torres, *Angew. Chem.* **119** (2007) 8510
12. B. O'Regan, M. Grätzel, *Nature* **353** (1991) 737

13. A. Hagfeldt, G. Boschloo, L. C. Sun, L. Kloo, H. Pettersson, *Chem. Rev.* **110** (2010) 6595
14. S. Eu, T. Katoh, T. Umeyama, Y. Matanoa, H. Imahori, *Dalton Trans.* **40** (2008) 5476
15. H. Imahori, T. Umeyama, S. Ito, *Acc. Chem. Res.* **42** (2009) 1809
16. P. Y. Reddy, L. Giribabu, C. Lyness, H. J. Snaith, C. Vijaykumar, M. Chandrasekharam, M. Lakshmikantam, J.-H. Yum, K. Kalyanasundaram, M. Grätzel, M. K. Nazeeruddin, *Angew. Chem. Int. Ed.* **46** (2007) 373
17. J. H. Yum, S. R. Jang, R. Humphry-Baker, M. Grätzel, J.-J. Cid, T. Torres, M. K. Nazeeruddin, *Langmuir* **24** (2008) 5636
18. V. Aranyos, J. Hjelm, A. Hagfeldt, H. Grennberg, *J. Porphyrins Phthalocyanines* **5** (2001) 609
19. D. R. Boston, J. C. Bailar, Jr., *Inorg. Chem.* **11** (1972) 1579
20. F. Matemadombo, N. Sehlotho, T. Nyokong, *J. Porphyrins Phthalocyanines* **13** (2009) 986
21. N. Masilela, T. Nyokong, *Dyes Pigm.* **84** (2010) 242
22. L. C. Liu, C. C. Lee, A. T. Hu, *J. Porphyrins Phthalocyanines* **5** (2001) 806
23. Y. Ma, E. Vileno, S. L. Suib, P. K. Dutta, *Chem. Mater.* **9** (1997) 3023
24. L. Giribabu, Ch. Vijay Kumara, V. Gopal Reddy, P. Yella Reddy, Ch. Srinivasa Rao, S.-R. Jang, J.-H. Yum, M. K. Nazeeruddin, M. Grätzel, *Sol. Energ. Mat. Sol. C.* **91** (2007) 1611
25. W. Xu, B. Peng, J. Chen, M. Liang, F. S. Cai, *J. Phys. Chem. C* **112** (2008) 874
26. M. S. Liao, J. D. Watts, M. J. Huang, *Inorg. Chem.* **44** (2005) 1941
27. U. Mazur, K. W. Hipps, *J. Phys. Chem. C* **103** (1999) 9721
28. J. Krzystek, J. Telser, L. A. Pardi, D. P. Goldberg, B. M. Hoffman, L. C. Brunel, *Inorg. Chem.* **38** (1999) 6121
29. G. P. Shaposhnikov, V. E. Maizlish, V. P. Kulinich, *Russ. J. Gen. Chem.* **75** (2005) 1480
30. G. Li, K. J. Jiang, Y. F. Li, S. L. Li, L. M. Yang, *J. Phys. Chem. C* **112** (2008) 11591
31. D. P. Hagberg, J. H. Yum, H. J. Lee, F. D. Angelis, T. Marinado, K. M. Karlsson, R. Humphry-Baker, L. C. Sun, A. Hagfeldt, M. Grätzel, M. K. Nazeeruddin, *J. Am. Chem. Soc.* **130** (2008) 6259.